Int. J. Electrochem. Sci., 12 **(2017)** 455 – 465, doi: 10.20964/2017.01.18

International Journal of
ELECTROCHEMICAL
SCIENCE
www.electrochemsci.org

Sol-Gel Combustion Synthesis of $Li_{1.2}Mn_{0.54}Ni_{0.13}Co_{0.13}O_2$ as Cathode Materials for Lithium Ion Batteries

Dingzeng He, Qixun Guo, Hao Yin, Juntao Li, Zhengliang Gong*

College of Energy, Xiamen University, Xiamen 361005, P.R. China
*E-mail: qxguo@xmu.edu.cn

Received: 8 September 2016 / *Accepted:* 11 November 2016 / *Published:* 12 December 2016

Nanocrystalline $Li[Li_{0.2}Mn_{0.54}Ni_{0.13}Co_{0.13}]O_2$ cathode materials are successfully prepared by sol-gel combustion method with urea as both chelating agent and fuel. The effects of calcining temperature and solvent on the electrochemical performance are studied. The as prepared samples are characterized and tested by means of XRD, SEM and electrochemical methods. The electrochemical tests indicate that the materials synthesized at 800°C with water solvent deliver a high initial discharge capacity of 255.8 $mAhg^{-1}$, and a capacity retention of 76.8% after 50 cycles at a current density of 20 mAg^{-1} between 2.0 and 4.8 V vs. Li/Li^+. It also shows better rate capability compared with the materials calcined at 750°C, 850°C as well as the materials using alcohol solvent calcined at 800°C. The experimental results show that enhanced electrochemical performance of the materials calcined at 800°C with water solvent is due to the uniformly distributed nanoparticles with a shorter diffusion path, perfect crystallinity, and ordered layered structure including less cations mixing.

Keywords: Li-rich layered oxide, Sol-gel combustion, Lithium-ion batteries, Cathode materials

1. INTRODUCTION

Lithium-ion batteries (LIBs) with substantially enhanced energy density are now actively pursued as the most viable power sources for next-generation portable electronics, electric vehicles(EVs) and hybrid electric vehicles (HEVs), and even for grid-scale power storage applications.[1, 2] At present, $LiCoO_2$ is the most broadly applied commercial cathode materials for lithium-ion batteries because of its low technology process, favourable electrochemical cycling stability, and accredited specific capacity [3, 4]. The relatively high cost, high use of Co (which is scarce), toxicity and the expectation of large specific capacity have, therefore, resulted in the study of other possible substitutions.[4-7] Among them, lithium-rich layered oxides (LLOs) with the chemical formula of $xLi_2MnO_3 \cdot (1-x)LiMO_2$ (M= Ni, Co, Mn, Fe, Cr, $Ni_{1/2}Mn_{1/2}$, $Ni_{1/3}Co_{1/3}Mn_{1/3}$, …) have

drawn our much attention on account of their high discharge capacity (230–300mAh g^{-1}) and moderate average discharge voltage (above 3.6 V). [8, 9] It has been testified that the high discharge capacity of LLOs is due to the activation and concurrently transformation of Li_2MnO_3 component into another active component manganese dioxide (MnO_2) when the LLOs electrodes are charged to 4.5 V or higher. What's more, the product MnO_2 could be considered as a structural stabilizer to strengthen the cycling stability of another component $LiMO_2$ even at a wide-voltage window (e.g. 2~4.8 V). [10]

Moreover, electrochemical property of cathode materials validly rely on their particle size and morphology. [11] The cathode materials with nanoscaled particles demonstrated an enhanced rate capability because of large specific surface area. [12, 13] Concurrently, the synthesis approaches will greatly influence the particle size and morphology. At present, many methods have been applied to synthesize $xLi_2MnO_3\cdot(1-x)LiMO_2$, such as co-precipitation [14], microwave heating [15],sol-gel [16], ion-exchange reaction [17] and solid reaction [18]. In addition, combustion method has already been successfully applied to synthesize cathode materials with the fuel of sucrose [19], urea [20], PVA [21], citric acid [22], gelatin [23] and so on [24]. The Li-rich cathode material $Li_{1.2}Mn_{0.54}Ni_{0.13}Co_{0.13}O_2$ was usually synthesized by co-precipitation [25, 26]，but seldom reported by other methods. The method of sol-gel combustion aims at combining sol-gel process with low temperature combustion, which is a simple, cost-effective approach of producing $Li_{1.2}Mn_{0.54}Ni_{0.13}Co_{0.13}O_2$ with short preparation period as well as precise controlling of chemical reation ratios and reaction conditions. The urea can be acted as fuel and chelating agent for sol-gel combustion synthesis to produce submicron particles due to the quantity of heat generated at low temperature and the dispersion of the crystal nucleus while suppressing crystal growth at the same time. In the present work, we used simple sol-gel combustion synthesis to prepare$Li_{1.2}Mn_{0.54}Ni_{0.13}Co_{0.13}O_2$ with good cycling property and excellent rate capability as a cathode material for lithium-ion batteries. We study the structural characteristics and electrochemical properties of $Li_{1.2}Mn_{0.54}Ni_{0.13}Co_{0.13}O_2$ prepared at different temperature and with different solvent. As far as we know, this is the first report that explains the sol-gel combustion synthesis factor of a Li-rich $Li[Li_{0.2}Mn_{0.54}Ni_{0.13}Co_{0.13}]O_2$ layered cathode material.

2. EXPERIMENTAL

2.1. Sample Preparation and Characterization.

A simple sol-gel combustion method was used for the synthesis of $Li_{1.2}Mn_{0.54}Ni_{0.13}Co_{0.13}O_2$. Stoichiometric amounts of $Ni(NO_3)_2\cdot6H_2O$(1.26g), $Co(NO_3)_2\cdot6H_2O$(1.26g), $LiNO_3$(2.84g), $Mn(CH_3CO_2)_2\cdot4H_2O$(4.43g), NH_2CONH_2(14.68g) were dissolved in 30 ml water. Among them, 3 wt% excess $LiNO_3$ was added to compensate the lost during sintering treatment. The solution was stirred continuously at 80°C in water bath until a viscous blue gel was obtained after evaporation of the excess water. Then the gel was burned at 400°C for 15min in the pre-heated muffle furnace. Soon afterwards, the precursor was ground in an agate mortar and sintered again for crytallisation at 750°C，800°C，850°C in air for 16h in muffle furnace to obtain the cathode materials. The samples were named as W750, W800, W850. For a comparative purpose to state the influence of solvents, the

$Li_{1.2}Mn_{0.54}Ni_{0.13}Co_{0.13}O_2$ nanoparticles were also prepared using the same procedure with alcohol as solvent and renamed as A800 in simplified form.

The morphologies of the synthesized powder were investigated by field-emission scanning electron microscopy (FESEM) on a Zeiss Supra 55 operated at 10 kV. Powder XRD patterns of each sample were collected in a Rigaku D/Max-IV X-ray diffractometer using Cu Kα radiation operated at 40 kV and 40 mA. Data were recorded at a scan rate of 10°/min, in the 2θ range from 10° to 90°.

2.2. Electrochemical Measurements.

The electrochemical measurements were performed using CR2025 coin-type cells. The electrodes were prepared by coating a slurry, which were containing 80% synthesized materials, 10% carbon black (BLACK PEARL 2000) used for conductive agent, 10% polyvinylidene fluoride (PVDF) as binder mixed in an N-methyl-2-pyrrolidone (NMP) solvent, onto an aluminum foil and dried in vacuum for 12 h at 100 °C. The CR2025 coin-type cells were assembled in Argon-filled glove box (Labmaster100, Mbraun, Germany) with the cathodes as-prepared, metallic lithium foil as counter electrode, Cellgard 2300 film as separator and 1M LiPF6 dissolved in ethyl carbonate (EC) and dimethyl carbonate (DMC) (1:1 in volume) as electrolyte. The charge-discharge experiments were performed galvanostatically between 2.0 and 4.8V on a Land-CT2001 A battery tester (Wuhan, China) at 30 °C. The CR2025 cells were measured at various C rates (0.1, 0.2, 0.5, 1.0, 2.0 and 5.0 C) to investigate the rate capability of the synthesized materials (1 C rate corresponding to $200mA{\cdot}g^{-1}$). The cyclic voltammograms were tested by coin cell on a CHI660D electrochemical workstation at a scanning rate of 0.1 $mV{\cdot}s^{-1}$ with the voltage ranging from 2.0 V to 4.8 V.

3. RESULTS AND DISCUSSION

The powder XRD patterns of cathode materials synthesized by sol-gel combustion method under different conditions are shown in Fig. 1. The peaks of all patterns can be indexed as the a-$NaFeO_2$ layered structure with space group R-3m, except for the small peaks between 20° and 24°, which corresponding to the reflections of super lattice. The weak reflections from 20° to 24° for the sintered products, are in agreement with the Li, Mn, Ni cations arrangement that happens in the transition metal layers of Li_2MnO_3 region [27]. There are no impurity phases that can be detected in all samples. It is worth noting that some tiny differences in XRD patterns can be observed between the samples of using different solvents. The ordering of the materials structure is indicated by the XRD patterns with the I(003)/I(104) intensity ratio, the splitting degree of (006)/(102) and (108)/(110) [28]. As we can see from the Fig.1, the splitting of the (006)/(102), (018)/(110) peaks becomes stronger as the calcination temperature increases, suggesting that calcining temperature have a significant influence on the structure of the samples.. The relative intensity of I(003)/I(104) can be applied to estimate the extent of the cation mixing, which is one of the major issues that hinder the electrochemical property of Li-rich cathode layered materials. For the samples W800, A800,

I(003)/I(104) are 1.22 and1.26, respectively, higher than the intensity ratios for the other samples (such as 0.95 and 1.09 for W750 and W850), indicating that the less disordering of the structure of materials calcinated at 800°C. The ratio of I(003)/I(104) is similar for W800 and A800, indicating that the solvent has no significant influence on the ordering of the structure. Hence, the calcination temperatures applied during sol-gel combustion synthesis progress play an more important role in preparing materials with well-crystallized layered structures. What's more, the particle size is W750<A800<W800<W850 in order, calculated by the Scherrer formula.

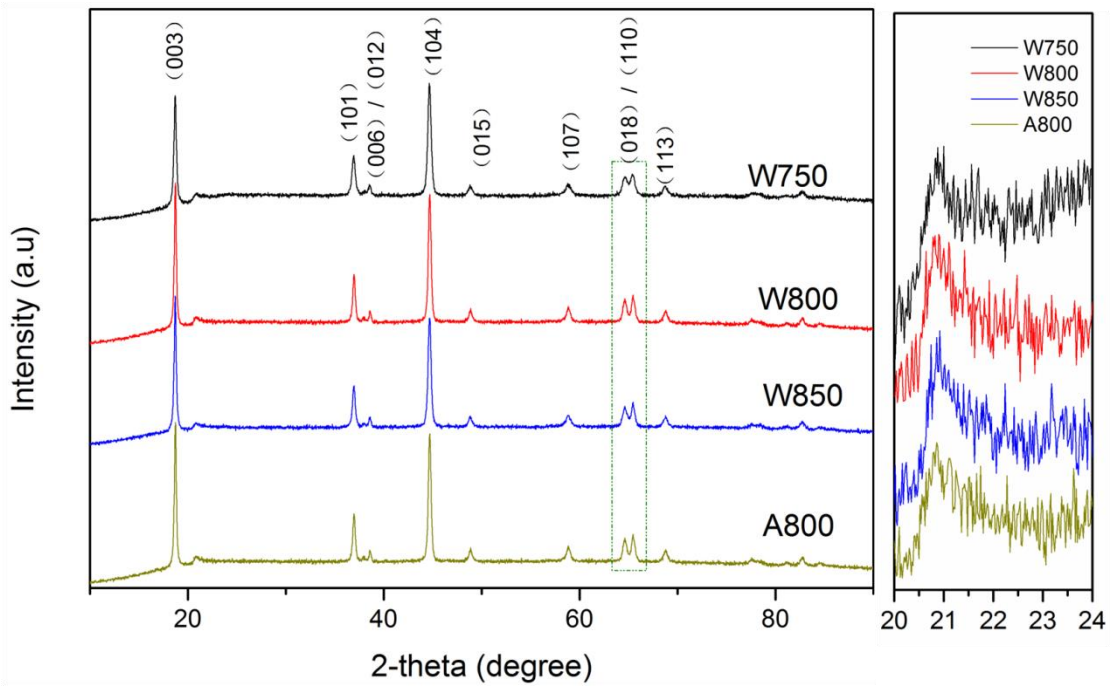

Figure 1. XRD patterns of the four $Li_{1.2}Mn_{0.54}Ni_{0.13}Co_{0.13}O_2$ samples: W750, W800, W850, A800 and the enlarging pictures of the XRD patterns from 20º to 24º.

SEM was performed to investigate the morphology of the $Li_{1.2}Mn_{0.54}Ni_{0.13}Co_{0.13}O_2$ samples. As shown in Fig. 2(a-d), the four samples have nano-porous structure. In whole, the partical dispersibility of W800 is better than that of W750, W850, and A800. All the samples are accompanied with different degree of aggregation obviously. A close observation at higher magnification, as show in the inset in (a), (b), (c), (d), uncovers a similar morphology as nanoparticals with different sizes (from 100 nm to 400 nm) and smooth surface. Sample W800 appears as homogeneously distributed particles with well-defined morphologies. We can conclude that the morphology of the materials synthesized by sol-gel combustion, is not only influenced by the temperature, but also by the solvent.

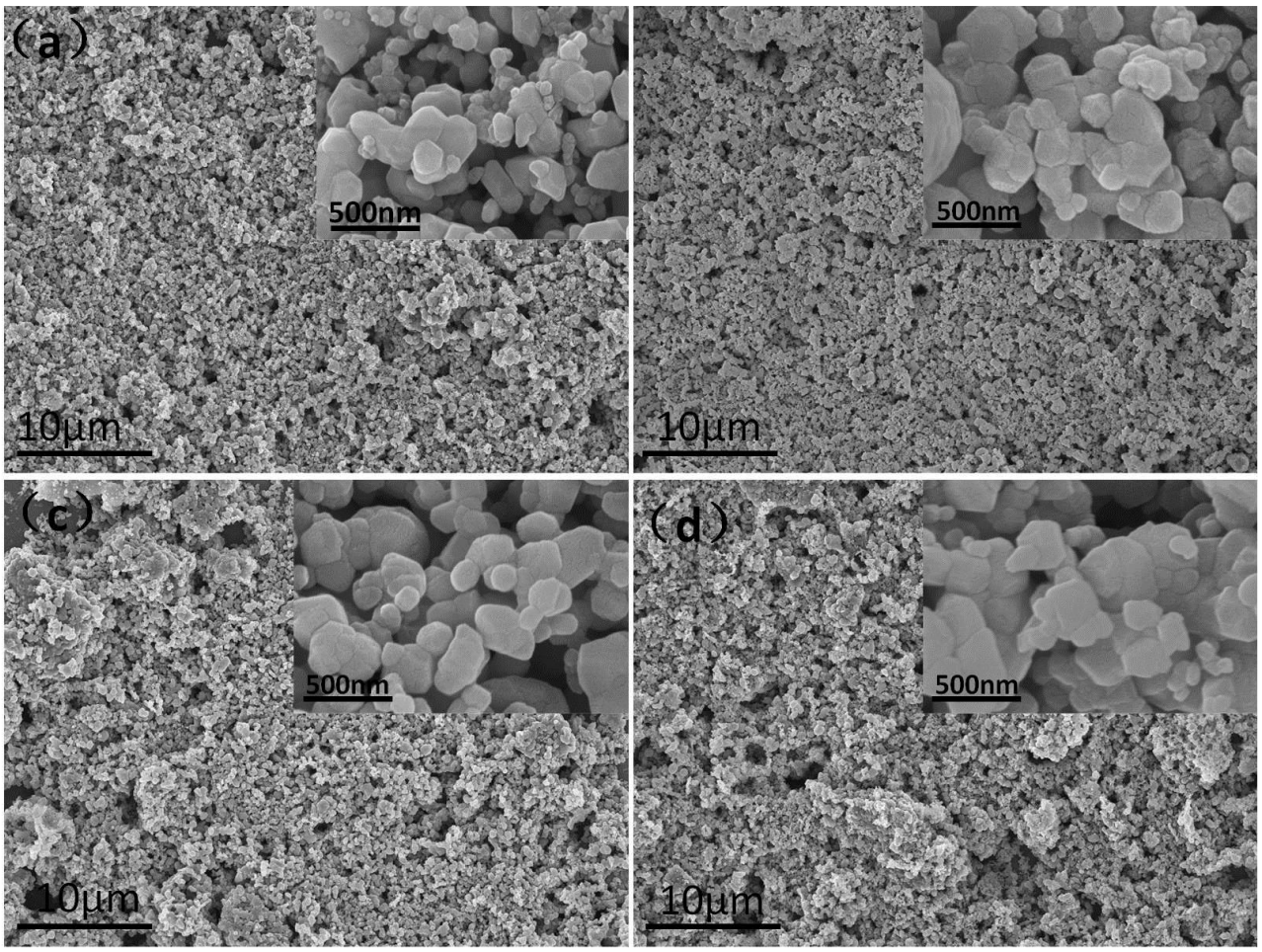

Figure 2. SEM images of the four $Li_{1.2}Mn_{0.54}Ni_{0.13}Co_{0.13}O_2$ samples: (a)W750, (b)W800, (c)W850, (d)A800, corresponding magnification factor is 2.27k and the embedded pictures in (a), (b), (c),(d) corresponding magnification factor is 59.97k.

The initial charge-discharge curves of four $Li_{1.2}Mn_{0.54}Ni_{0.13}Co_{0.13}O_2$ samples at 0.1C rate are shown in Fig.3. The four curves are in complete agreement with the electrochemical performance of Li_2MnO_3-$LiNi_xCo_yMn_{1-x-y}O_2$ type lithium-rich layered oxides [29]. Apparently, the first charge capacity of Li-rich cathode material can be separated into two parts. The charge capacities of the initial charge reaction below 4.4 V, which is associated with lithium extraction from $LiNi_{1/3}Co_{1/3}Mn_{1/3}O_2$ component accompanying with the oxidation of Ni2+ and Co3+, are almost the same for electrodes prepared by different methods. In addition, the long voltage plateau at approximately 4.5V is attributed to the electrochemical activation of Li_2MnO_3 component in the layered cathodes accompanied with Li^+ and oxygen ions extraction from the host. Above-mentioned two voltage plateaus are in good agreement with the oxidation peaks at about 4.0 V and 4.6 V observed in CV curves (Fig6). In Fig.3, the intial discharge capacity of W800 is 255.8mAhg^{-1}, which is higher than 212, 241.3 and 245.5 mAhg^{-1} for W750, W850 and A800, respectively. Furthermore, the columbic efficiencies of the four electrodes (W800, W750, W850, and A800) are 76.31%, 68.2%, 74.58% and 75.35%, respectively. The higher columbic efficiency of W800 can be partially attributed to the less cation mixing and better layered structure which corresponds with the XRD results.

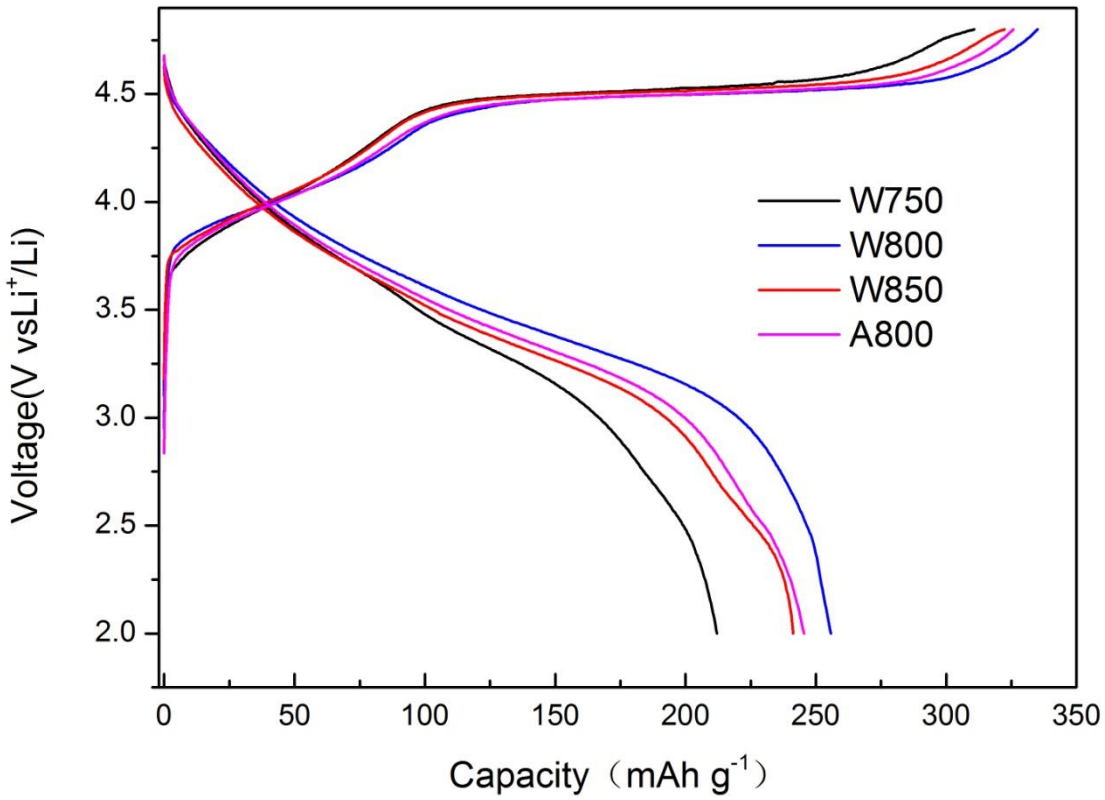

Figure 3. the initial charge/discharge curves of the four $Li_{1.2}Mn_{0.54}Ni_{0.13}Co_{0.13}O_2$ samples: W750, W800, W850, A800.

Fig.4 presents the cycle performance of $Li_{1.2}Mn_{0.54}Ni_{0.13}Co_{0.13}O_2$ at 0.1C and 1C. For 1C, the cells were first cycled at 0.1C for 2 cycles to activate the Li_2MnO_3 component and then cycled at 1C in the following cycles. The sample W800 shows a reversible capacity of 193.7, 151.8 $mAhg^{-1}$ after 50 cycles for 0.1C and 1C, respectively, which are higher than 141.2 and 107.8 $mAhg^{-1}$ for W750, 177.0 and 110.7 $mAhg^{-1}$ for W850, and 171.2 and 124.7 $mAhg^{-1}$ for A800. Obviously the reversible capacity is increased first and then decreased for the cathode materials with the improved calcining temperature from 750°C to 850°C at both 0.1C and 1C. The reason may be that low temperature results in poor crystallininty and high temperature generates large particles and a certain degree of aggregation. All of these could hinder lithium transport and lead to poor cyclability. No matter at 0.1C or 1C, the cyclability of the W800 is better than the A800. The water solvent is in favor of raw material dispersion and manufacturing uniform cathode material. The capacity retention is 76.8% and 87.4% at 0.1C and 1C after 50 cycles, respectively. There are two major arguments to interpretation the capacity degradation. One is the dissolution of the metal ions, particularly the manganese ion during the charge –discharge process. The other one is the Jahn-Teller distortion during the cycling process. [30, 31]

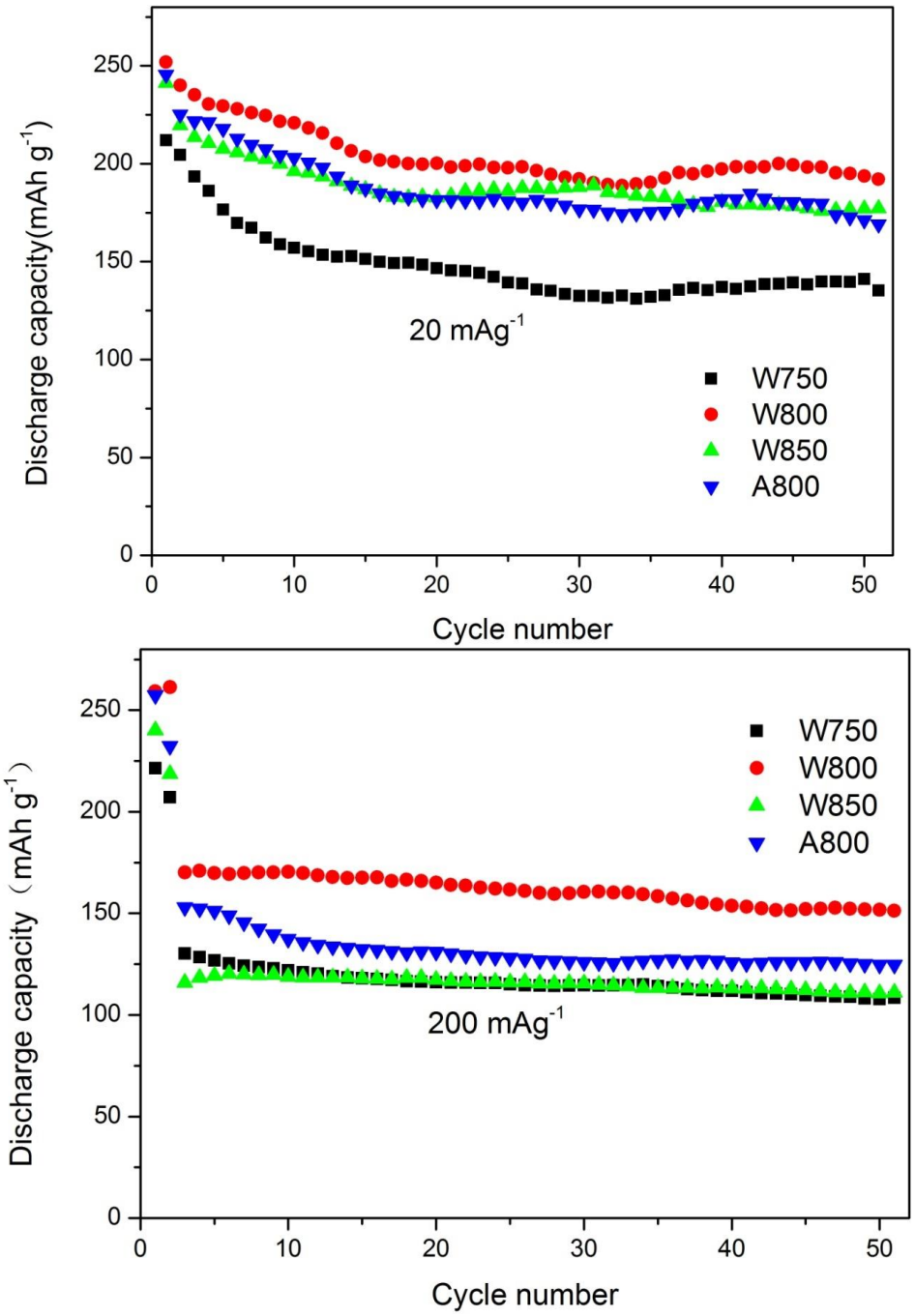

Figure 4. Cycle property of the four $Li_{1.2}Mn_{0.54}Ni_{0.13}Co_{0.13}O_2$ samples: W750, W800, W850, A800 at different current densities.

Fig.5 shows the rate capability of the $Li_{1.2}Mn_{0.54}Ni_{0.13}Co_{0.13}O_2$ samples from current density 0.1C to 5C. It can be seen that the $Li_{1.2}Mn_{0.54}Ni_{0.13}Co_{0.13}O_2$ prepared in the water solvent at 800℃ displays higher capacity and better rate performance than the samples prepared under other conditions. W800 delivers the discharge capacities of 264.1, 219.5, 183.7, 154.0, 122.0 and 65.0 $mAhg^{-1}$ at current densities 0.1C, 0.2C, 1C, 2C and 5C, respectively. However, W750, W850, A800 exhibits poor rate capability, the discharge capacities are only 49.3, 47.6 108.5 mAg^{-1} at high rate of 2C, respectively. The rate performance of W800 and A800 are similar. Then we can conclude that calcining temperature

have more significant influence on the rate performance of the samples, relative to the solvent. It should be noted that the poor rate capability of W750 and W850 is related to the cation mixing in the Li-layers, the poor crystallinity of W750, and the large particles and aggregation of W850. For lithium-rich material, small particles will short the diffusion path of lithium and electron and benefit to the electrochemical properties. A great extent of cations mixed in the layered cathode materials suggests more cations in the Li layer, which could impede lithium transport and result in poor rate properties and poor cyclability. As a whole, the nature conductivity of Li-rich layered oxide is poor, and the transformation from $xLi_2MnO_3 \cdot (1-x)LiMO_2$ to Li_xMO_2(M=Mn,Co,Ni) will mess the well-formed lattice, resulted in low lithium transport.[32]. At the same time, this is the direction of our later research. At different rates, the difference of capacity between the samples is about 80 $mAhg^{-1}$, which suggests 800℃, in water, is effective to sol-gel combustion synthesize Li-rich layered cathode materials with high rate performance.

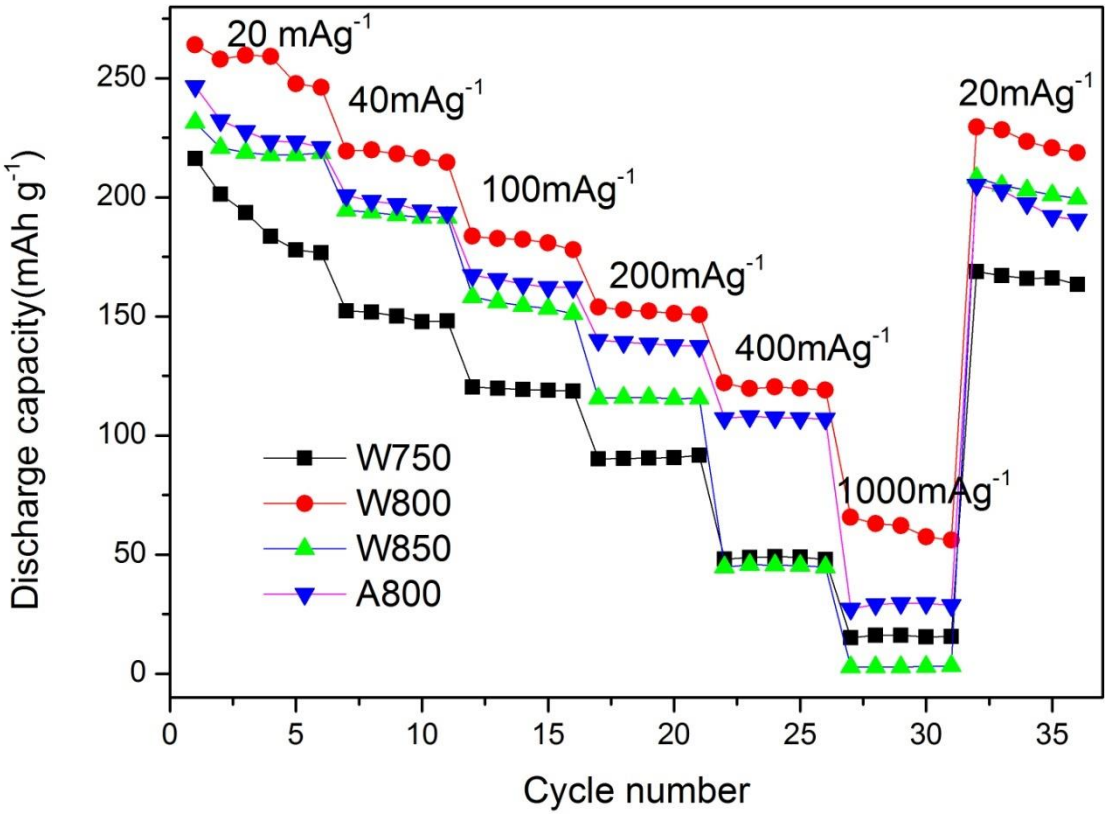

Figure 5. Rate performance of the four $Li_{1.2}Mn_{0.54}Ni_{0.13}Co_{0.13}O_2$ samples: W750, W800, W850, A800,the half cells were charged and discharged at the same current densities.

Fig.6 shows the CV curves of sample W800 for the previous three cycles. In this CV picture, we can see two high anodic peaks. The first anodic peak at about 4.0 V in the first cycle is primarily because of the partial oxidation of Ni^{2+} to Ni^{4+}. The second peak at higher potential (4.5~4.8 V) is associated predominantly with the cobalt oxidation from Co^{3+} to Co^{4+} and the irreversible electrochemical activation reaction that extracts Li_2O from the Li_2MnO_3 component to take shape MnO_2 [33]. For the reason that the second anodic peak at higher potential vanishes or reduces to very low in the following cycles, the great irreversible capacity is rightly reflected by the second large

anodic peak over 4.5 V in the initial CV cycle. There are two obvious cathodic peaks in the discharge process. Although it is unlikely to distinguish the reduction courses of the individual Co, Mn and Ni from the curve, it can be supposed from the theoretical analysis that the course at approximate 4.5 V may be contacted with the possession of tetrahedral sites by lithium in the wide delithiated layer and the lower voltage processed at about 3.25 V to the possession of octahedral sites, consistent with the studies of Hayley et al [34]. The two courses still arise at the third cycle, and the conclusion that both of the reaction processes are reversible can be testified.

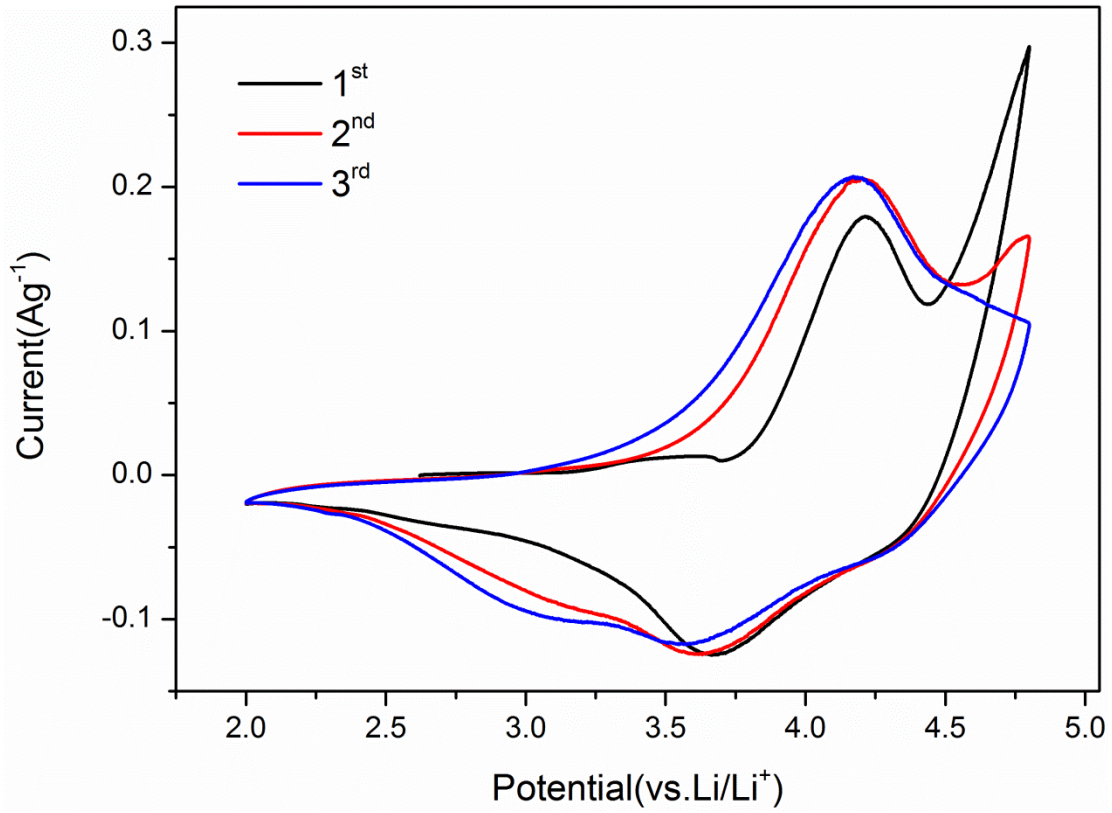

Figure 6. Cyclic voltammetry curves of the $Li_{1.2}Mn_{0.54}Ni_{0.13}Co_{0.13}O_2$ sample of W800 for the initial three cycles (the scan rate is 0.1mV s^{-1} and voltage range is 2-4.8V)

4. CONCLUSIONS

The high capacity cathode materials $Li_{1.2}Mn_{0.54}Ni_{0.13}Co_{0.13}O_2$ have been successfully prepared by sol-gel combustion reaction. The effects of solvent and calcining temperature on the structure and electrochemical properties were investigated. The $Li_{1.2}Mn_{0.54}Ni_{0.13}Co_{0.13}O_2$ obtained from different temperatures and solvents all display Li_2MnO_3-$LiMO_2$ type layered structure. The particle size is W750<A800<W800<W850 in order, calculated by Scherrer formula. As lithium ion battery cathodes, the W800 displays higher discharge capacity, better cycling stability and rate capability. Particularly, it exhibits a higher initial discharge capacity and coulombic efficiency of 255.8 $mAhg^{-1}$ and 76.31% at 0.1C. It also shows high capacity retention of 76.8% and 87.4% at 0.1C and 1C after 50 cycles. The effects of solvent and calcining temperature on the morphology and structure match well with the

electrochemical properties. Overall, the results obtained suggest that both solvent and calcining temperature, especially the calcining temperature play important roles in the synthesis of $Li_{1.2}Mn_{0.54}Ni_{0.13}Co_{0.13}O_2$. Suitable calcining temperature and solvent effectively improved the electrochemical property properties of the $Li_{1.2}Mn_{0.54}Ni_{0.13}Co_{0.13}O_2$ synthesized by sol-gel combustion. The materials prepared by sol-gel combustion method are promising cathode materials for rechargeable lithium ion batteries. In the paper, we found the optimum condition for sol-gel combustion synthesis $Li_{1.2}Mn_{0.54}Ni_{0.13}Co_{0.13}O_2$. Then the following research will be devoted to further improve the rate capability and cycle stability.

ACKNOWLEDGMENTS
The project is sponsored by the Scientific Research Foundation for the Returned Overseas Chinese Scholars, State Education Ministry (Batch No. 44) and the Natural Science Foundation of Fujian Province (No.2010J05034).

References

1. X.Y. Lai, J.E. Halpert, and D. Wang, *Energy. Environ. Sci*., 5 (2012) 5604.
2. B. Kang, and G. Ceder, *Nature*., 458 (2009) 190.
3. D.D. M. Neil, Z. Lu, and J.R. Dahn, *J. Electrochem. Soc*., 149 (2002) 1332
4. K. Mizushima, P.C. Jones, P.J. Wiseman, and J.B. Goodenough, *Mater.Res. Bull.*, 15 (1980) 783.
5. K.K. Lee, W.S. Yoon, K.B. Kim, K.Y. Lee, and S.T. Hong, *J. Power Sources*., 97 (2001) 308.
6. S.B. Majumder, S. Neito, and R.S. Katiyar, *J. Power Source*s., 154 (2006) 262.
7. J.N. Reimers, E. Rossen, C.D. Jones, and J.R. Dahn, *Solid State Ionics*., 61 (1993) 335.
8. H.J. Yu, and H.S. Zhou, and J. Phys. *Chem. Lett*., 4 (2013) 1268.
9. Y. Bai, Y. Li, Y.X. Zhong, S. Chen, and F. Wu, C. Wu, *Prog. Chem*., 26 (2014) 259.
10. C.H. Zhao, X.X. Liu, X.R. Liu, H. Zhang, and Q. Shen, ACS Appl. *Mater.Interfaces*., 6 (2014) 2386.
11. C.X. Cheng, L. Tan, H.W. Liu, and X.T. Huang, *Mater. Res. Bull*., 46 (2011) 2032.
12. J.M. Amarilla, R.M. Rojas, F. Pico, L. Pascual, K. Petrov, D. Kovacheva, M.G. Lazarraga, I. Lejona, and J.M. Rojo, *J. Power Sources*., 174 (2007) 1212.
13. D. Kovacheva, H. Gadjov, K. Petrov, S. Mandal, M.G. Lazarraga, L. Pascual, J.M. Amarilla, R.M. Rojas, P. Herrero, and J.M. Rojo, *J. Mater. Chem*., 12 (2002) 1184.
14. B. Li, Y.Y. Yu, J.B. Zhao, *J. Power Sources*., 275 (2015) 64.
15. Q.W. Peng, Z.Y. Tang, L.Q. Zhang, and X.J. Liu, *Mater. Res. Bull*., 44 (2009) 2147.
16. S. Sivaprakash, and S.B. Majumder, *Solid State Ionics*., 181 (2010) 730.
17. D. Kim, S.H. Kang, M. Balasubramanian, and C.S. Johnson, *Electrochem. Commun*., 12 (2010) 1618.
18. S.J. Shi, J.P. Tu, Y.Y. Tang, Y.X. Yu, Y.Q. Zhang, and X.L. Wang, *J. Power Sources* .,221 (2013) 300.
19. J.M. Zheng, X.B. Wu, Y. Yang, *Electrochimica. Acta*., 56 (2011) 3071.
20. C.H. Zhao, Z.B. Hu, Z.H. Qiu, and K.Y. Liu, *Micro & Nano Letters*., 10 (2015) 662.
21. A. Subramania, N. Angayarkanni, and T. Vasudevan, *Mater. Chem. Phys*., 102 (2007) 19
22. P. Ghosh, S. Mahanty, R.N. Basu, and Mater. *Chem. Phys*., 110 (2008) 406.
23. P. Periasamy, and N. Kalaiselvi, *J. Power Sources*., 159 (2006) 1360.
24. P. Manikandan, M.V. Ananth, T.P. Kumar, M. Raju, P. Periasamy, and K. Manimaran, *J. Power Sources*., 196 (2011) 10148.

25. X.J. Guo, Y.X. Li, M. Zheng, J.M. Zheng, J. Li, Z.L. Gong, and Y. Yang, *J. Power Sources*., 184 (2008) 414.
26. C.S. Johnson, N. Li, C. Lefief, M.M. Thackeray, *Electrochem. Commun*., 9 (2007) 787.
27. K.A. Jarvis, Z. Deng, L.F. Allard, A. Manthiram, and P.J. Ferreira, *Chem. Mater.*, 22(2012) 11550.
28. Z.L. Gong, H.S. Liu, X.J. Guo, Z.R. Zhang, and Y. Yang, *J. Power Sources*., 136 (2004) 139.
29. H.Z. Zhang, Q.Q. Qiao, G.R. Li, S.H. Ye, and X.P. Gao, *J. Mater. Chem*., 22 (2012) 13104.
30. A. Ito, D. Li, Y. Sato, M. Arao, M. Watanabe, M. Hatano, H. Horie, and Y. Ohsaw, *J. Power Sources*., 195 (2010) 567.
31. J. Park, J.H. Seo, G. Plett, W. Lu, and A.M. Sastry, *Electrochem. Solid State Lett.*, 14 (2011) 14.
32. S.J. Shi, J.P. Tu, Y.Y. Tang, Y.X. Yu, Y.Q. Zhang, X.L. Wang, and C.D. Gu, *J. Power Sources*., 228 (2013) 14.
33. W. He, J. Qian, Y. Cao, X. Ai, and H. Yang, *RSC Advances*., 2 (2012) 3423.
34. H.H. Hayley, N. Yabuuchi, Y.S. Meng, S. Kumar, J. Breger, C.P. Grey, and Y. S. Horn, *Chem. Mater*.,19 (2007) 2551.